Acta Montanistica Slovaca
ISSN 1335-1788
actamont.tuke.sk

Identification of karstic zones using RS & GIS method, Fuzzy logic and AHP in Neka catchment, Mazandaran, Iran

Mohammad Ali GHOLI NATAJ MALEKSHAH[1], Davood JAHANI[2], Seyed Ramazan MOUSAVI[3], Nader KOHANSAL GHADIMVAND[4] and Seyed Hamid VAZIRI[5]*

Authors' affiliations and addresses:
[1]Department of Geology, North Tehran Branch, Islamic Azad University, Tehran, Iran.
e-mail: mgholinataj@yahoo.com

[2]Department of Geology, North Tehran Branch, Islamic Azad University, Tehran, Iran
e-mail: d.jahani26@gmail.com

[3]Department of Watershed Management, Faculty of Natural Resources, Sari Agriculture Sciences and Natural Resources University, Mazandaran Province, Iran.
e-mail: srm@sanru.ac.ir

[4]Department of Geology, North Tehran Branch, Islamic Azad University, Tehran, Iran
e-mail: n_kohansal_ghadimvand@iau_tnb.ac.ir

[5]Department of Geology, North Tehran Branch, Islamic Azad University, Tehran, Iran
e-mail: h_vaziri@iau_tnb.ac.ir

***Correspondence:**
Department of Geology, North Tehran Branch, Islamic Azad University, Tehran, Iran
tel.: 09121270836
e-mail: d.jahani26@gmail.com

Acknowledgement:
Thanks to the Advanced Remote Sensing Lab and GIS of the Sari Agricultural Sciences and Natural Resources University to support the perfect laboratory of remote sensing and GIS for software and data collaboration.

How to cite this article:
Gholi Nataj Malekshah,, M.A., Jahani, D., Mousavi, S.R., Kohansal Ghadimvand, N. And Vaziri, S.H.. Identification of karstic zones using RS & GIS method, Fuzzy logic and AHP in Neka catchment, Mazandaran, Iran. *Acta Montanistica Slovaca,* Volume 27 (3), 697-709.

DOI:
https://doi.org/10.46544/AMS.v27i3.10

Abstract
This study focuses on identifying zones and karstic phenomena using the RS & GIS method along with Fuzzy logic integration and the Hierarchical Analysis Process (AHP) in part of Neka catchment in Mazandaran province in the north of Iran. In this research, eight lithological factors, density and distance from the fractured lineaments, density and distance from the drainages, topographic slope, precipitation and vegetation status, were extracted from satellite and archival data as well as field data. Then these factors which affect karst formation and development are fuzzy and are weighted by the AHP method and integrated with T-norm, T-conorm (S-norm) and Compromise Operators. The results were processed by using software such as ArcGIS, ENVI, RockWorks, IDRISI, Expert Choice and PCI Geomatica, which were evaluated based on fieldwork. The results of this study show that most karst developments occurred in Lar Formation with the upper Jurassic. According to field visits, the best and most appropriate output for fuzzy layers integration are the use of a compromise operator in the range of 0.9 to 0.95. In spite of the suitable ability of Landsat 8 bands to extract lineaments due to vegetation status and other environmental conditions, the use of DEM was also necessary. This study shows that the use of new remote sensing and GIS technology, combined with Fuzzy logic and AHP, increases accuracy and speed and reduces cost in karst studies.

Keywords
AHP, Fuzzy logic, Iran, Karstic zones, Mazandaran, Neka catchment, Remote sensing and GIS.

Introduction

A composite image of all the roughness, shapes, pores, and phenomena caused by water corrosion, above and below the surface, in various soluble geological formations, is karst (Ford, 2007; LaMoreaux, 2001). Various factors are involved in the formation and spread of this diagenetic phenomenon, such as the type and degree of solubility of rocks, the physicochemical properties of running and submerging waters, climate, geomorphology, hydrologic and hydrogeological conditions, joints and fractures density and tectonic dynamics (Daoxian, 1997; Yu, 2016; Kaufmann, 2016; Lucia, 2007). The study and management of karst areas have long been the focus of geologists, hydrologists, geomorphologists, hydrogeologists, environmentalists, and even eco and geotourists (LaMoreaux, 2001; Dafny, 2015). Today, in spite of certain special conditions of karstic areas, such as water resources, environmental conditions and low-risk site selection for civil construction, identifying karst areas is particularly important (Uromeihy, 2000). On the other hand, due to the limited cost, time, number of experts, easy access, ground equipment and even the lack of clear karstic evidence in some field studies, we had to reduce these problems by using some methods. One of these efficient methods is the use of remote sensing (RS) technology. One of these efficient methods is the use of remote sensing technology. In this way, satellite images for various purposes have been produced based on the solar spectrum's reflection and its related laws (Ho, 2009; Tripathi, 2014). These images are processed and analyzed in RS & GIS software. For example, using thermal imagery data can detect lineaments such as fractures (Meijerink et al., 2007).

Today the use of new RS & GIS technologies in environmental studies, especially in geology, has particular importance, and due to ability, speed, accuracy and up-to-date data, these technologies in many important geosciences issues, including lithological and mineralogical studies (Mars, 2010; Yu, 2012), geological structures (Ruisi 2011), surface water status and quality, (NG Rostom et al., 2017; Ouma et al., 2018), geomorphological features (Radaideh 2016) and other land-related studies (Asadzadeh, 2016) are used. In addition to evaluating the effective factors in these studies (Neruda, 2015), it is possible to produce specialized maps with up to 90% accuracy (Mohammadizad, 2017).

New RS & GIS technology, coupled with accurate and varied satellite information such as LiDAR, IRS P6, Landsat, Aster, Worldview and SRTM, are being utilized in karst studies (Elez, 2013; Pei et al., 2018; Radaideh et al., 2016). In this method, while investigating karstic areas, based on the difference in air temperature near the surface (O'Driscol, 2006), the relationship of tectonic fabrics with water currents (Kresic, 1995), morphological characteristics (Litwin, 2008) and karstic shapes, especially sinkholes Uromeihy (2000), their range of development is also evaluated. In some cases, groundwater in karst areas can be identified by using this method (Alonso-Contes, 2011).

In this study, to identify karstic areas in Neka catchment, east of Mazandaran province, Iran, eight important factors affecting karst formation are the density of lineaments and drainages, the distance of lineaments and drainages, lithology, climate, and vegetation that were evaluated. On the other hand, by the widespread use and application of Fuzzy logic in many sciences, and especially in the earth sciences (Demicco, 2004), all of the upper mentioned effective factors have been fuzzed into separate layers in the GIS software environment, except lithology that is subject to the certainty of Boolean logic. The role of each of the influencing factors in this study is not identical and differs from one another. Therefore, we use the AHP method, which is one of the most efficient models in multi-criteria decision-making and is used to prioritize the effective factors in studies (Saaty, 1980) to determine the weight and coefficient of each layer.

There were various reasons to do this study. One of these reasons has been the promotion and development of karstic studies and identification by RS & GIS using Fuzzy logic and AHP in a dense vegetation area. Due to the dense vegetation of the Hyrcanian forest and the morphological conditions of the region, information on karstic phenomena is limited. Another reason for using this method was to determine the extent of karstic phenomena in the study area that the Hyrcanian forests in the north of Alborz Range in Iran are very wide, and identifying karst areas in this vast area by ordinary methods requires a great deal of time, cost and energy.

Materials and Methods

Study Area

The study area, which is part of the Neka catchment, is located in the eastern part of Mazandaran province and the northeast part of the central Alborz Range. It covers an area of 617 square kilometres and is located between longitudes 53°, 19°, 40° to 53°, 56°, 12° east, and latitudes 36°, 27°, 30° to 36°, 39°, 43° north (Figure 1). The general topographic slope is northwest, with the lowest elevation in the northwestern part at 50 m and its highest elevation in the southeast part at 2218 meters. The Hyrcanian has the highest density in the western half and the lowest density in the eastern half. The average annual rainfall is about 600 mm, with the highest rainfall in the western half and the lowest rainfall in the eastern half.

Geologically, part of the northern part is the Alpine-Himalayan orogenic belt in western Asia, according to structural geological divisions in the Alborz Zone (Stöcklin, 1968; Alavi, 1991; Nogole-Sadat, 1993), Alborz-

Azerbaijan Zone (Nabavi, 1976). Based on the sedimentary-structural divisions, it is located in central Iran (Aghanabati, 2004). Most of the rocks are Mesozoic and Cenozoic deposits, and metamorphic rocks are known as Gorgan Schists and are partially visible northeast of the area. Carbonate rocks such as limestone, dolomitic, and sandy limestone are widely spread, and even calcareous clastic rocks are observed.

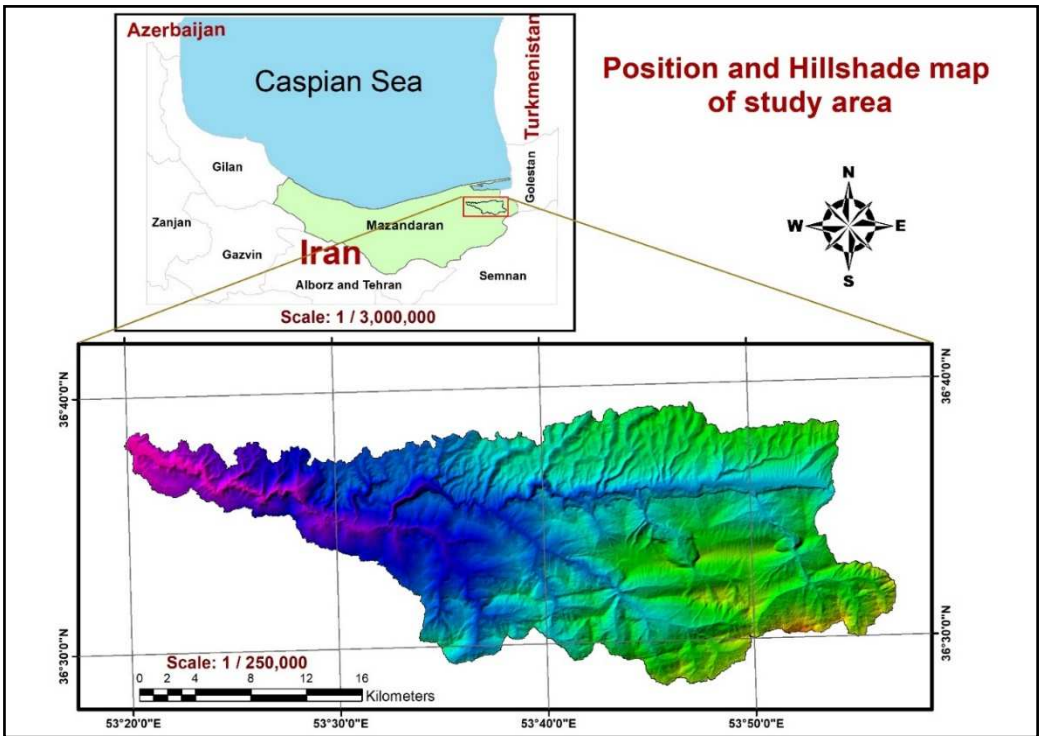

Fig. 1. Location of the study area at the global, provincial and local scale (created by authors).

Data used

Several different satellite data have been used, such as ASTER, LANDSAT 8, topographic maps, geological maps, climatology data, ASTER DEM and GPS data which can be seen in Table 1.

Tab. 1.List of data used

Type of data	Source
Landsat 8 (Row 35, Path 163)	USGS
ASTER (Row 35, Path 163 and Row 34, Path 163)	USGS
Geological maps(1:100000)	Geological Survey of Iran
Topographic maps(1:25000)	Iranian Surveying Organization
Meteorological stations data	Meteorological Organization of Mazandaran
GPS data	Field-working
ASTER DEM	Produced from ASTER paired stereo images

Methodology

In this research, several different satellite data have been collected. Then it was needed to pre-process and treat the generation of criterion raster maps such as lithological characteristics, density and distance from lineaments, vegetation, climate, density and distance from drainages and slope. Also, the post-process has been done, such as Fuzzy logic and AHP and combined them. Finally, we have generated potential karst maps over the area (Figure 2).

Due to the extensive vegetation, the use of satellite data to extract lithological features was not sufficient, and, therefore, geological maps have been used to determine the lithological composition. Fieldworks surveys have also been assisted to match this data. These maps have been extracted and georeferenced in a GIS environment (Fig. 3A).

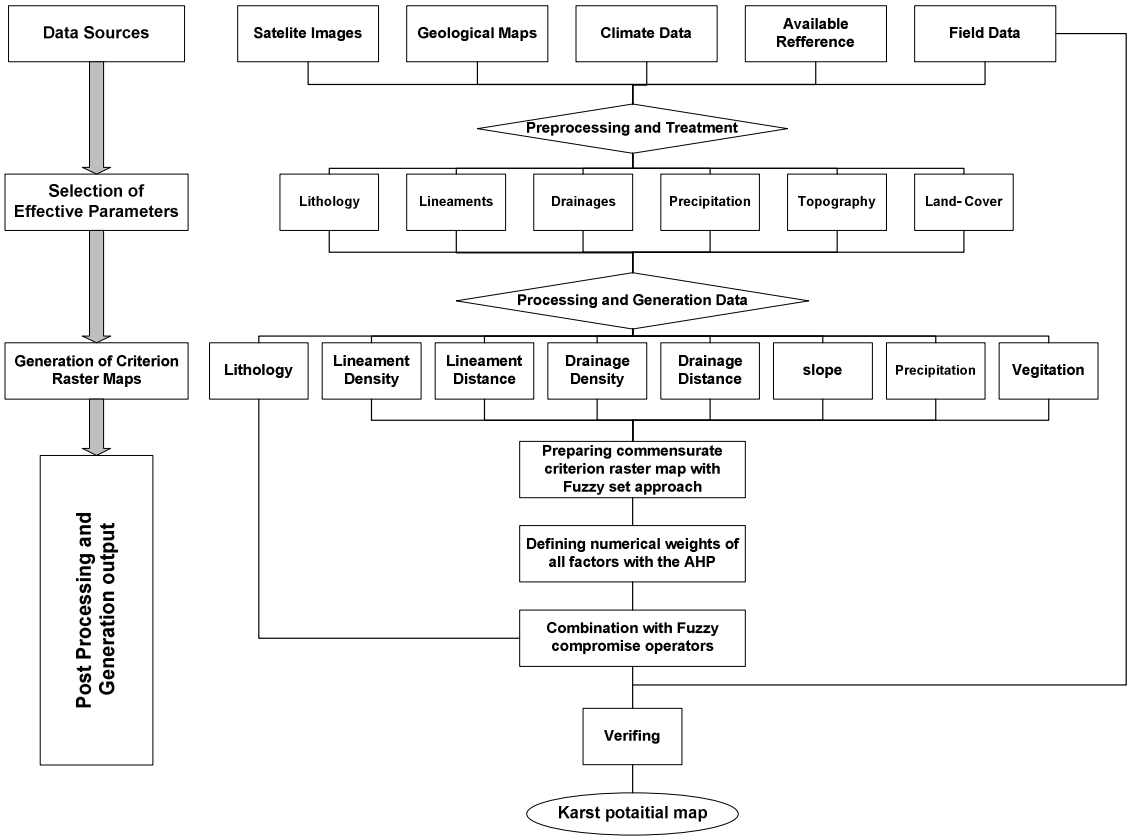

Fig. 2. Flowchart Steps of this research. (created by authors).

Because of the widespread usage of the ASTER Digital Elevation Model (ASTER DEM) in this research, we have generated it by using PCI Geomatica software. In producing DEM by photogrammetric techniques, ASTER paired stereo images were used based on parametric variables of Internal Orientation, External Orientation and Ground Control Points (GCPs) (Balik et al., 2004).

Three manual, automatic and semi-automatic methods have been used to extract lineaments. In manual mode, High Pass filters, Principal Component Analysis (PCAs) and colour combinations can be highlighted to extract lineaments. For filtering of Band 4 of Landsat 8, it has been used Gradient-Robert, Gradient-Sobel and Gradient-Prewitt methods. By processing bands and reducing their size, PCA can be very useful in highlighting images and making it easier to extract lineaments.

In the automatic extraction of lineaments, the three used algorithms are Haar Transform, Hough Transform and Segment Tracing Algorithm (STA) (Kocal 2004). The Line module in PCI Geomatica software, which is reasonably close to the STA algorithm, can be useful in automatically extracting lineaments. In the STA algorithm, linear pixels are automatically detected based on their grey degree difference and then converted to vectors (Koike et al., 1995).

In the process of extracting lineaments, linear effects are first extracted from an image; then, they are recorded as vectors according to the six parameters RADI, GTHR, LTHR, FTHR, ATHR and DTHR in this module. In this study, these parameters are used to extract lineaments from Band 4 of Landsat 8, which are generally more capable of distinguishing between geological features and vegetation status. At this stage, several line maps have been generated by changing the values of the six parameters. In this area, due to the vegetation status and many land uses and also the existence of a clear boundary between farms and forests, some lineaments have been identified as non-fault and fractured. Therefore, continuing to extract these lineaments has been used DEM and finally, by integrating and overlaying the manual and automatic outputs, a single supervised lineament map has been prepared. Then, the lineaments density maps (Fig. 3B) and the distances to these lineaments (Fig. 3C) were prepared in the GIS software environment. Rockwork software was also used to produce the rose diagram based on its length and density.

The Normalized Difference Vegetation Index (NDVI) is used to identify and extract vegetation status after performing the pre-processing of the OLI sensor data (Table 2) because chlorophylls in plants have the highest absorption in blue (0.4 - 0.5 μm) and red (0.6 - 0.7 μm) spectra, and their highest reflectance occurs in green (0.5 - 0.6 μm) spectra. Therefore, the NDVI index is based on Near Infrared (NIR) and Red Band bands (Equation 1).

$$NDVI = (NIR - Red) / (NIR + Red) \quad (1)$$

In Landsat 8 images, this index is given by equation 2 and bands 4 and 5 are used.

$$\boldsymbol{NDVI} = (\boldsymbol{Band\ 5} - \boldsymbol{Band\ 4}) / (\boldsymbol{Band\ 5} + \boldsymbol{Band\ 4}) \quad (2)$$

Tab. 2. Name of bands, wavelength and resolution in Landsat 8.

Band	Landsat 8 Operational Land Imagers (OLI) & Thermal Infrared Sensor (TIRS)		
	Band Name	Wavelength (micrometers)	Resolution (meter)
Band 1	Ultra-Blue	0.435-0.451	30
Band 2	Blue	0.452-0.512	30
Band 3	Green	0.533-0.590	30
Band 4	Red	0.636-0.673	30
Band 5	NIR	0.851-0.879	30
Band 6	SWIR 1	1.566-1.651	30
Band 7	SWIR 2	2.107-2.294	30
Band 8	Panchromatic	0.503-0.676	15
Band 9	Cirrus	1.363-1.384	30
Band 10	TIRS 1	10.60-11.19	100 * (30)
Band 11	TIRS 2	11.50-12.51	100 * (30)

To derive the status of the drainages, DEM generated with 15 m accuracy of ASTER data was used in the GIS environment. In this software environment, ArcHydro extensions were used, and then the maps of drainage density (Fig. 3E) and the distances to the drainage (Fig. 3F) were generated.

The topographic slope of the area was calculated based on degree and mapped by DEM using GIS software (Figure 3G).

To determine the climatic condition of the region, the weather data were obtained from the General Meteorological Department of Mazandaran Province, and through interpolation, isothermal, isohyetal and isoevaporation curves were generated on an annual average. To determine the type of climate, the De Matron method based on equation 3 was used, and the climatic characteristics map of the study area was prepared (Fig. 3H).

$$\boldsymbol{I = P/(T + 10)} \quad (3)$$

In this equation, *I*, *P* and *T* are the coefficients of drought, mean annual precipitation in mm, and mean annual temperature in °C, respectively.

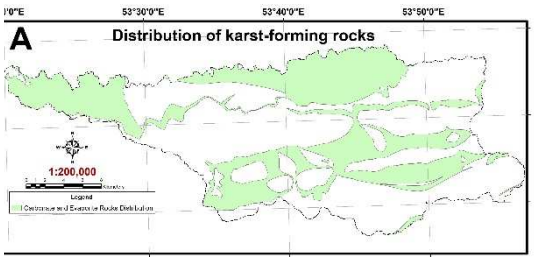

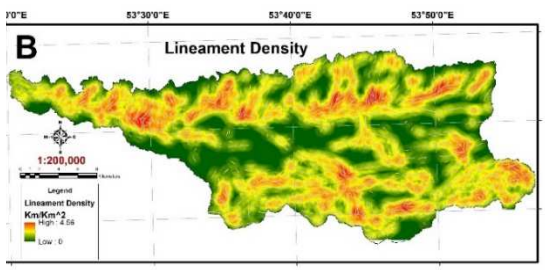

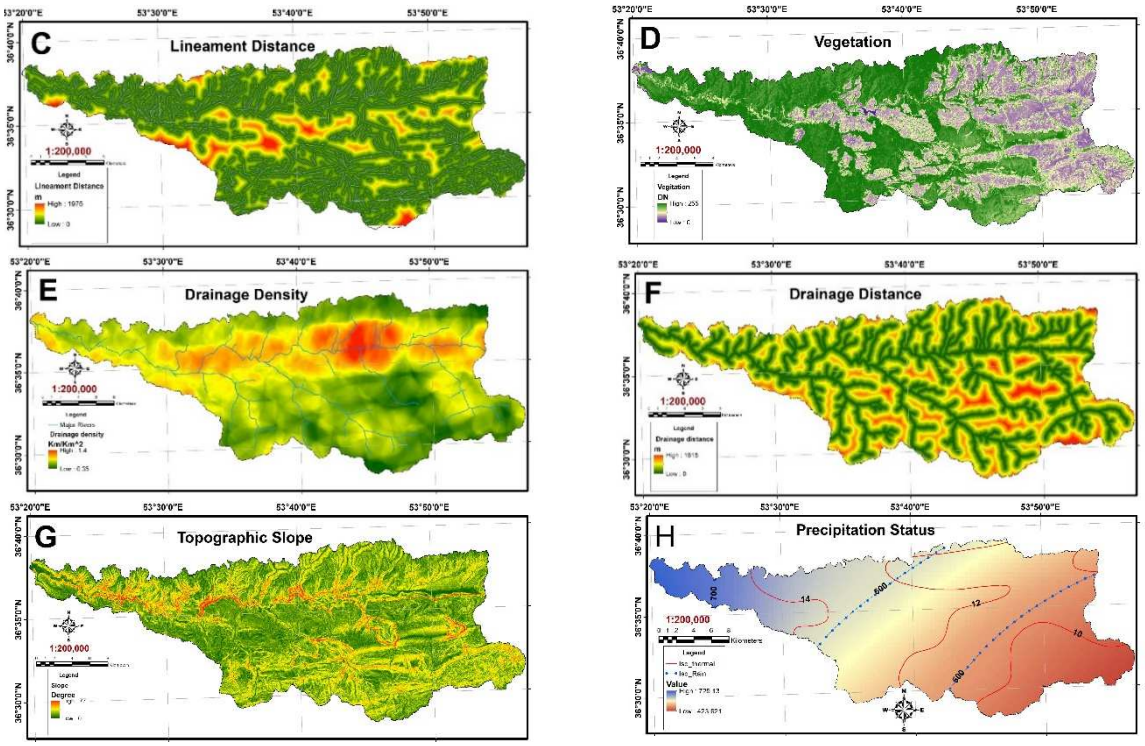

Fig. 3. Eight features effective in karst formation and extension in the study area; (A) shows the distribution of karst-forming rocks, (B) fracture lineament density, (C) lineaments distance, (D) vegetation density status from dense to grassland, (E) density of major and minor drainages, (F) distance from major and minor drainages, (G) topographic slope changes, and (H) precipitation status(created by authors).

Results and Discussion

Since Fuzzy logic is now widely used in many sciences, especially in geoscience, due to its ability to produce appropriate outputs (Demicco, 2004), we have used this logic in order to obtain more relevant and acceptable results based on the purpose of this research.

A fuzzy set is a set of data with an uncertain boundary, unlike ordinary sets that have a defined boundary. In cases where the boundaries of two or more societies are definitely separated from each other, according to Boolean logic, the membership rate of each sample to each community will be zero or one.

In integrating layers of information, it is essential to consider the value of each layer and its units. Because the criteria for the information layers are different. For example, this study used units of meters for height and distance, per cent for density and degree for slope.

On the other hand, in the decision-making model, the layers can integrate that their criteria have comparable and proportional units. Otherwise, there is ambiguity, and it cannot be classified. In the Fuzzy logic, the data of each layer in the study area, based on the target type, receive a membership value indicating its desirability. In other words, each pixel with a higher membership degree is more desirable. In fuzzy mapping, in addition to determining the degree of membership, it is important to select the type of fuzzy function that depends on the research goals and the data criteria of each layer (Demicco, 2004).

In this study, fuzzy sets were determined for each of the slope layers, the density of lineaments and drainages, distance from drainages and lineaments, vegetation and precipitation whose data have an uncertain boundary. For example, as we know, the density of lineaments is directly related to karst. So in the fuzzy approach, the linguistic expression "high density of lineaments", which is a qualitative expression, is a fuzzy set. This linguistic expression is converted to a membership number of 0 to 1, and its function will be linear. In this example, the membership value of one is for pixels with a density greater than 1.4 km / km^2, and the membership value of zero is for pixels with a density less than 0.4 km / km^2 of the lineament. However, pixels with a lineaments density of between 0.4 and 1.4 km / km^2 have a gradual membership rate of 0 to 1. For the purposes of this study, for each layer with uncertain boundary data, the degree of fuzzy membership with linear function has been defined (Fig. 4). Next, the pixel values of each previously extracted layer are calculated in GIS based on its fuzzy membership function, and new raster layers are produced (Figure 5). However, the lithology with definite boundaries (soluble and non-soluble rocks) is based on the uncertainty problem in Boolean logic. In other words, pixels with solubility and karsting, value 1 and other pixels are assigned numeric value 0.

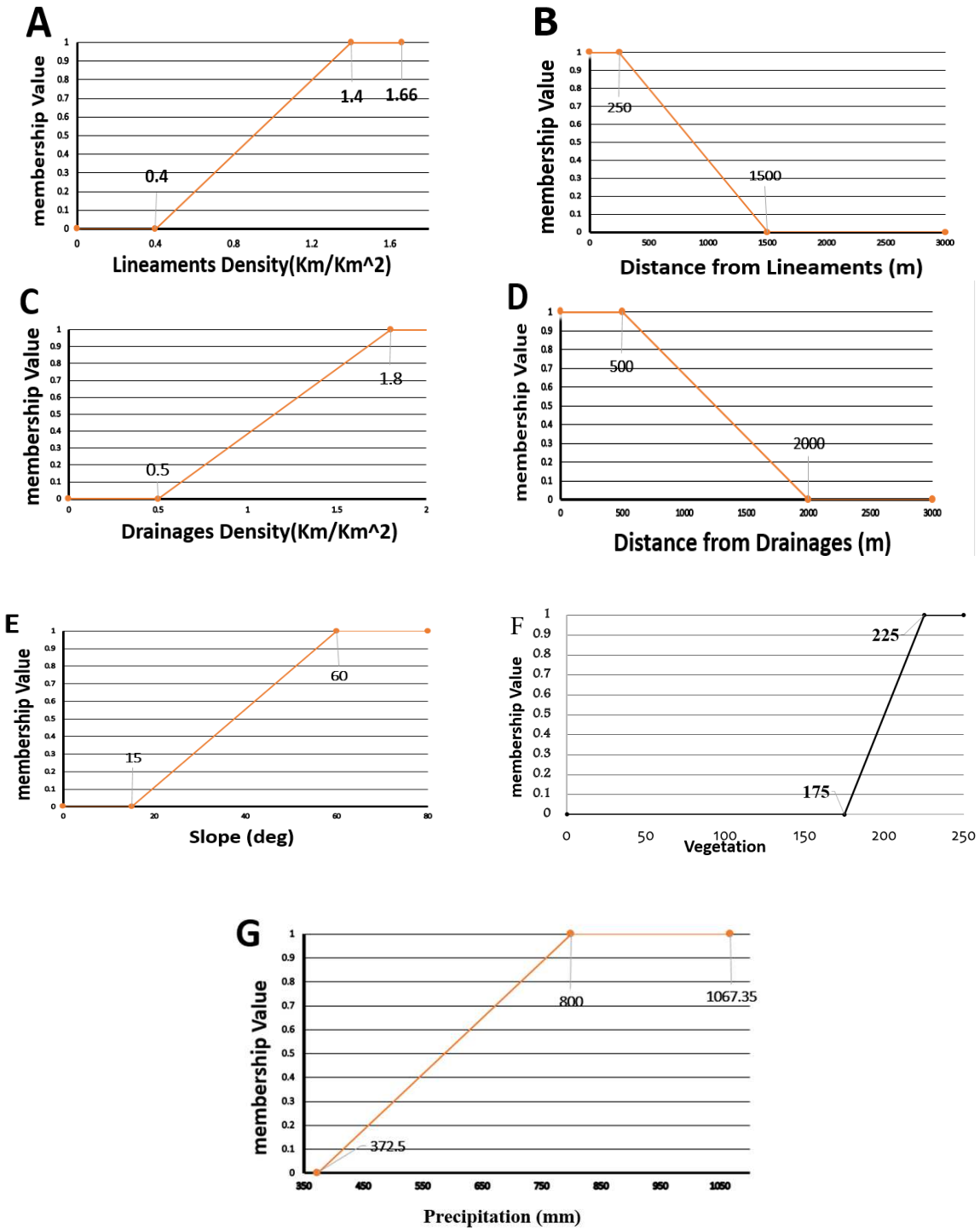

Fig. 4. Fuzzy membership degree graphs of data with uncertain boundaries in this study as (A) lineaments density, (B) distance from lineaments, (C) drainages density, (D) distance from drainages, (E) slope, (F) vegetation and (G) precipitation (created by authors).

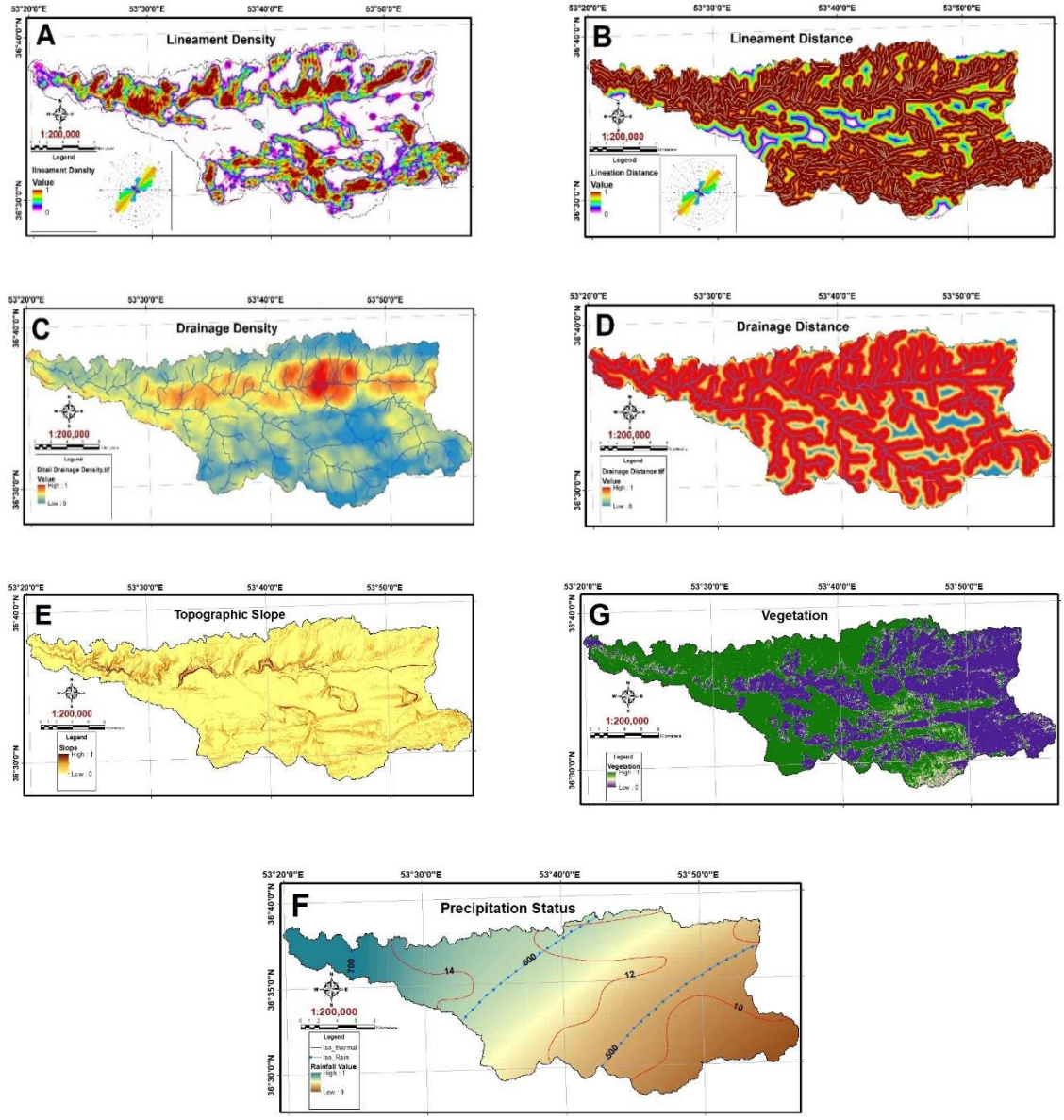

Fig. 5. Fuzzy logic maps based on membership degree set for data with uncertain boundaries in this study; (A) lineaments density, (B) lineaments distance, (C) drainages density, (D) drainages distance, (E) Topographic slope (F) Vegetation and (G) precipitation status(created by authors).

Another important factor in calculating and measuring the layers is determining the weight of each layer based on the purpose of the research. The roles of each of the influencing factors in the studies are not the same. In this study, the effect of the extracted octahedral layers on the formation of karst phenomena is not the same. Therefore, their effectiveness must be determined. Accordingly, we used the AHP method to determine the weight and coefficient of each layer and then applied them to our calculations.

The AHP method, which is one of the most efficient models in multi-criteria decision making and is used to prioritize the effective factors in the studies, includes a weighting matrix based on binary comparisons between the effective factors and the amount of participation and thus the weight of each criterion is determined (Saaty, 1980). The Analytical Hierarchy Process method, while employing a large number of effective factors, can apply the experts' views on the effectiveness of the factors and calculate the criterion inconsistency index based on the judgments made (Saaty, 1998; Changa et al., 2007).

In this study, to determine the preference of eight factors influencing karst phenomena and convert the oral judgments of some experts into quantitative experts, we prepared a matrix table using Analytical Hierarchy Process in Expert Choice software and made pairwise comparisons (Table 3). Then the efficacy weight of each parameter is calculated with the incompatibility coefficient of less than 1% (Figure 6). In this calculation, the weight of

lithology effectiveness is 0.302, lineament density 0.170, lineament distance 0.225, drainage density 0.071, drainage distance 0.107, precipitation 0.032, topographic slope 0.071, and vegetation 0.021.

Tab. 3. Pairwise comparisons matrix of eight effective factors in karst formation and extension in the study area based on the AHP process.

	Lithology	Lineament Density	Lineament Distance	Drainage Density	Drainage Distance	Rainfall	Slope	Vegetation
Lithology	1	2	2	5	4	7	5	7
Lineament Density		1	-2	4	3	5	2	6
Lineament Distance			1	5	3	6	3	7
Drainage Density				1	-2	3	2	5
Drainage Distance					1	4	3	6
Rainfall						1	-4	3
Slope							1	6
Vegetation	Inconsistency: 0.06							1

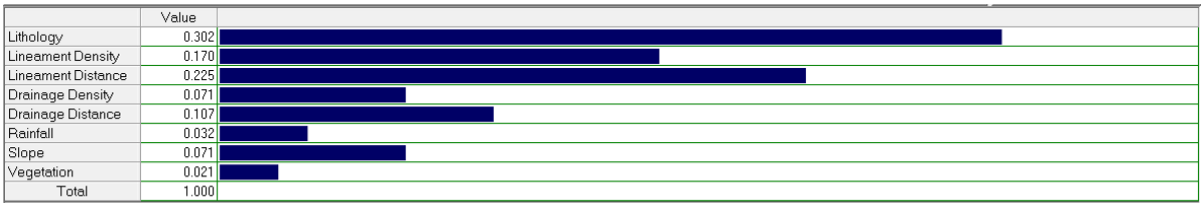

Fig. 6. Expert Choice software output histogram of the effective weight of each of the parameters affecting karst formation and expansion in the study area based on the AHP process with less than one per cent incompatibility coefficient (created by authors).

The next step in this study was the integration of fuzzied raster layers and the effective weight calculated by the AHP method for each factor. For this purpose, the Weighted Linear Combination method was used. This method is one of the most commonly used methods of data integration, especially in land use, sustainability analysis, site selection and resource evaluation (Malczewski et al., 2000). In this method, each factor is multiplied by its weight, and then the factors are aggregated. Finally, the required maps are extracted (Equation 4).

$$\boldsymbol{Ai} = \sum_{\boldsymbol{i}} \boldsymbol{Wj} \,.\, \boldsymbol{Xij} \tag{4}$$

In this equation, A_i is the karst exponential, the computational factor X_i, and the factor weight W_j.

There are several cumulative operators on fuzzy sets to optimally combine these sets to produce a single fuzzy set. These different operators can be divided into three categories: T-norm, T-conorm (S-norm) and compromise operator (Mohammadi, 2013):

A - T-norm operator

μ combination ≤ Min (μA, μB, μC, . ..)

μ combination: degree of cumulative membership

The most common use of this operator is Standard intersection and Algebraic product, and their equation is as follows.

Standard intersection: μcombination = Min μA, μB, μC, . . .)

Algebraic product: μcombination =$\prod_{i=1}^{n} (\mu i)$

B - S-norm operators

μ combination = Max (μA, μB, μC, . . .)

The most common uses of these types of operators are Standard union, probability intersection and algebraic sum.

Standard union: μcombination = Max (μA, μB, μC . . .)

Algebraic sum: μcombination = 1 - $\prod_{i=1}^{n} (\mu i)$

C -compromise operator

μ combination = Max (μA, μB, μC, . . .)
The operator is an agreement between the T-norm and S-norm operators and includes the γ operator. The γ operator is:
Min (μA, μB, μC, . . .)$\leq \mu$ combination $\leq$ Max (μA, μB, μC, . . .)

In this equation, γ changes from zero to one. If γ is zero, the combination of this operator is equal to the Fuzzy Algebraic product, and if γ is 1, the combination of this operator will be the Fuzzy Algebraic sum. Accordingly, the outputs of the gamma operator are flexible (Carter and Graem, 1991).

In this study, a compromise operator was used. Based on multiple field visits from the study area, the best and most appropriate output for the layer cumulation will be in the range of γ between 0.9 and 0.95 (Figures 7B and 7C) and, in less and more than this range, the accuracy of extracting karst features is reduced (Figures 7A and 7D).

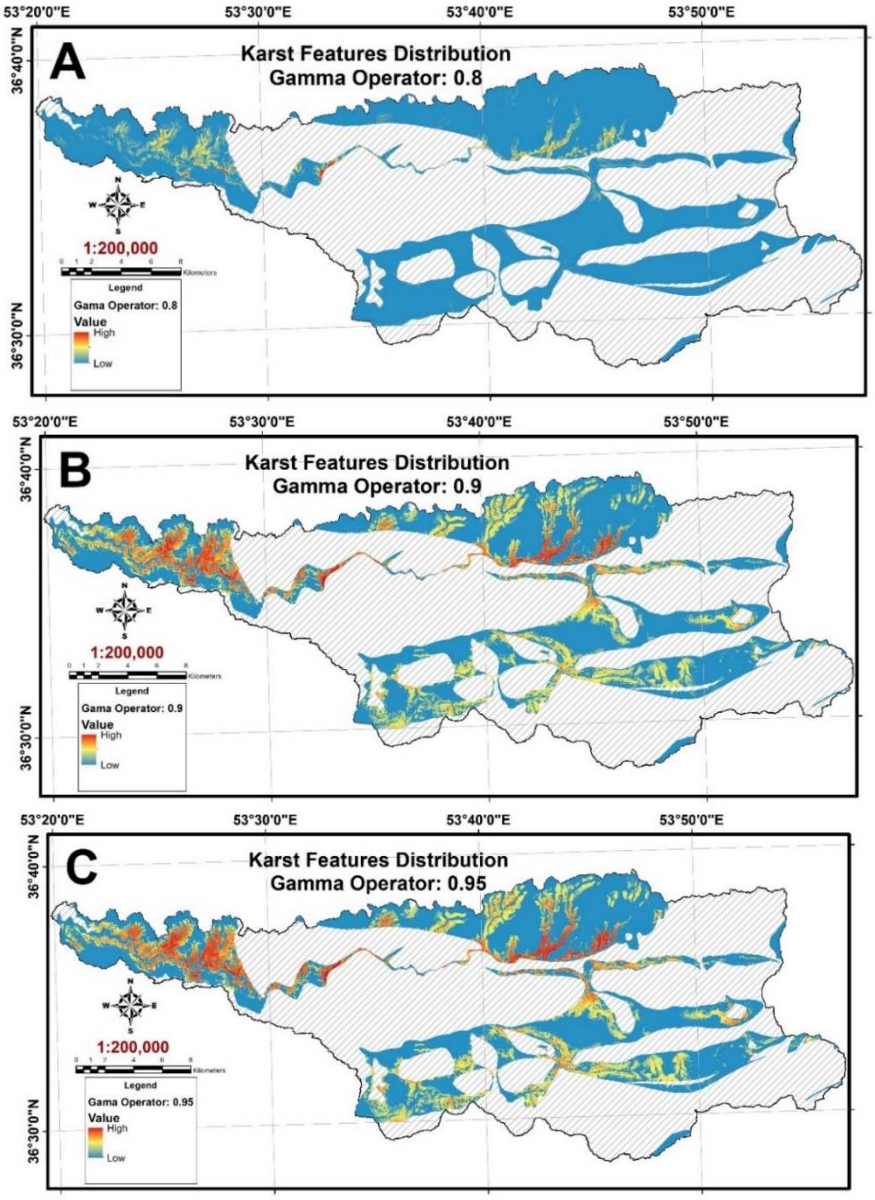

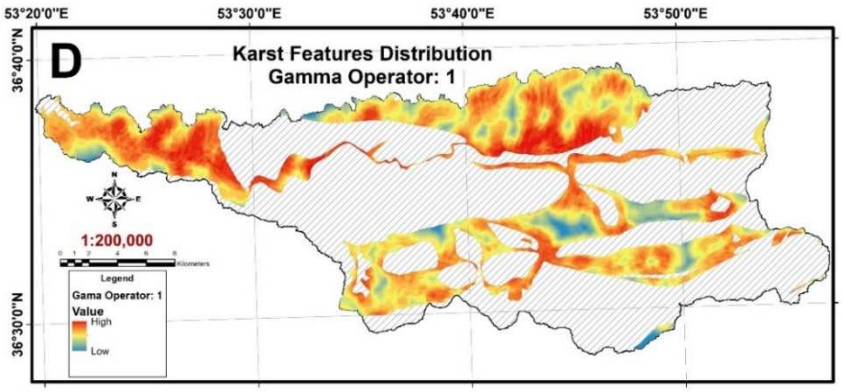

Fig. 7. Maps produced based on cumulative fuzzy layers using compromise operator. (A) γ = 0.8, (B) γ = 0.9, (C) γ = 0.95 and (D) γ = 1. The best and most appropriate output for the layer cumulation will be in the range of γ between 0.9 and 0.95(created by autours).

Conclusion

Nowadays, due to different methods of identifying areas with karstic features as one of the most important geological and environmental phenomena, using RS & GIS combined with Fuzzy logic and AHP can be one of the appropriate tools in this activity. Due to the accuracy, speed and cost reduction in the study process, this method can be well-positioned. This study selected eight factors of lithology, density and distance from fracture lineaments, density and distance from drainages, topographic slope, precipitation and vegetation status as influencing factors on karst formation and development. According to the results of the AHP, the most and the least weight factors affecting the identification of karstic zones, respectively, are karst-forming rocks and vegetation status. Fuzzy logic has been used in this study to combine the effective factors with multiple units and achieve more desirable results. Some of the results of this study are:

- The most developed karst phenomenon in the Upper Jurassic limestone (Lar Formation) has occurred in the northwestern part of the study area.
- In the northern part of the study area, where Lower Cretaceous Micritic limestones were distributed, karst development is more subjected to fracture lineaments and then emerged as deep and narrow canals with continuing karstic activity.
- In the central and southern parts of the study area, karstification is less intense in Paleocene sandy limestone. However, due to the low thickness of this rock unit (average 10 m) and the influence of running water, karstification has resulted in the formation of east-west karstic windows, and the upper Cretaceous marl rock unit has appeared.
- According to multiple field visits from the study area, the T-norm and T-conorm (S-norm) cumulative operators on fuzzy sets did not have good output, while the best and most appropriate output for the layer cumulation has occurred in the range that γ is between 0.9 and 0.95.
- In this area with a high diversity of vegetation with multiple land uses, lineament extraction should be done in three - manual, automatic and semi-automatic methods. Also, using Landsat 8 images to extract lineaments is inappropriate, and DEM should also be assisted.
- Using Fuzzy logic and hierarchical analysis process (AHP) in karst study can lead to acceptable results that are closer to reality based on field observations.
- RS & GIS are more economized in karst studies in this area due to their speed, accuracy and easy access to data. Due to the wide range of areas with relatively similar environmental conditions, it is necessary to use this method further.

References

Agha- Nabati, A. (2004). Geology of Iran. *Geological Survey of Iran*. (In Persian).

Alavi, M. (1991). Sedimentary and Structural Characteristics of the Paleo-Tethys Remnants in Northeastern Iran. *Geology Society of American*, 103, 983.

Asadzadeh, S. & De Souza Filho, C.R. (2016). A review on spectral processing methods for geological remote sensing, *International Journal of Applied Earth Observation and Geoinformation*, Vol. 47, 69-90.

Balik, F., Alkis, A., Kurucu, Y., & Alkis, Z. (2004). Validation of radargrametric DEM generation from RADARSAT images in high relief areas in Edrimit region of Turkey. *The international archives of the photogrammetry*, remote sensing and spatial information science, 34, 30.

Changa, K.F., Chiangb, C. M., & Chouc, P.C. (2007). Adapting aspects of GB Tool 200 searching for suitability in Taiwan, *Building and Environment*, 42:310–316.

Carter, B., & Graem F. (1991). Geographic information system for geoscientists: modelling with GIS. *Pergamon*, Ontario, pp 319–470.

Dafny, E., Tawfeeq, K.J., & Ghabraie, K. (2015). Evaluating temporal changes in hydraulic conductivities near karst-terrain dams: Dokan Dam (Kurdistan-Iraq), *Journal of Hydrology*, Vol. 529, 265-275.

Daoxian, Y. (1997). Sensitivity of karst process to environmental change along the Pep II transect, *Quaternary International*, Vol. 37, 105 – 113.

Demicco, R.V., & George, J. K. (2004). *Fuzzy Logic in Geology*, Elsevier Science, 347p.

Elez, J., Cuezva, S., Fernandez-Cortes, A., Garcia-Anton, E., Benavente, D., Cañaveras, J.C., and Sanchez-Moral, S. (2013). A GIS-based methodology to quantitatively define an Adjacent Protected Area in a shallow karst cavity: The case of Altamira cave, *Journal of Environmental Management*, Vol. 118, 122-134.

Ford, D. & Williams, P. (2007). Karst Hydrogeology and Geomorphology, John Wiley & Sons Ltd, 562 P.

Ho, P.G.P. (2009). *Geoscience and Remote Sensing*, In-The pub., 598 p.

Kaufmann, G., & Romanov, D. (2016). Structure and evolution of collapse sinkholes: Combined interpretation from physico-chemical modelling and geophysical field work, *Journal of Hydrology*, Vol. 540, 688-698.

Kresic, N. (1995). Remote Sensing of Tectonic Fabric Controlling Groundwater Flow in Dinaric Karst, *Remote Sensing Environ*, Vol. 53, 85-90.

Kocal, A. (2004). A Methodology for Detection and Evaluation of Lineaments from Satellite Imagery, Ms. thesis, Middle East Technical University, 121 p.

Koike, K., Nagano, S. & Ohmi, M. (1995). Lineament Analysis of Satellite Images Using A Segment Tracing Algorithm (STA), *Computers and Geosciences* , Vol. 21, No. 9, 1091-1104.

LaMoreaux, P.E. (2001). Living with karst, *CLB Printing Company*, 64p.

Litwin, L., & Andreychouk, V. (2008). Characteristics of high-mountain karst based on GIS and Remote Sensing, *Environ. Geol*, Vo;. 54, 979-994.

Lucia, F.J. (2007). Carbonate Reservoir Characterization, *Springer-Verlag Berlin Heidelberg*, Second Edition, 336 P.

Malczewski, J. (2000). On the Use of Weighted Linear Combination Method in GIS: Common and Best Practice Approaches, *Transactions in GIS*, 4(1): 5-22.

Mars, J.C., & Rowan, L.C. (2010). Spectral assessment of new ASTER SWIR surface reflectance data products for spectroscopic mapping of rocks and minerals, *Remote Sensing of Environment*, Vol. 114, 2011-2025.

Meijerink, A.M.J., Bannert, D., Batelaan, O., Lubczynski, M.W., & Pointet, T. (2007). Remote sensing applications to groundwater, by the United Nations Educational, *Scientific and Cultural Organization*, Printed in France, 311P.

Mohammadi, Z., Alijani, F. & Rangzan, K. (2013). DEFLOGIC: a method for assessment of groundwater potential in karst terrains: Gurpi Anticline, southwest Iran. *Arab J,* Geosci. 17.

Mohammadizad, R., & Arfania, R. (2017). Advanced Investigation of Remote Sensing to Geological Mapping of Zefreh Region in Central Iran, *Open Journal of Geology*, 2017, 7, 1509-1529.

Nabavi, M.H. (1976). An introduction to the geology of Iran, *Geological survey of Iran*. (in Persian)

Neruda, p. (2015). GIS analysis of the spatial distribution of Middle Palaeolithic artefacts in Kulna Cave (Czech Republic), *Quaternary International*, 1-19 1040-6182/© 2015 Elsevier Ltd and INQUA. All rights reserved.

Nogole-Sadat, M.A.A., & Almasian, M. (1993). Tectonic Map of Iran in 1:1000000 Scale. *Geological Survey of Iran*, Tehran.

O'Driscol, M.A., & DeWalle, D.R. (2006). Stream–air temperature relations to classify stream–ground water interactions in a karst setting, central Pennsylvania, USA, *Journal of Hydrology*, Vol. 329, 140-153.

Ouma, Y.O., Waga, J., Okech, M., Lavisa, O., & Mbuthia, D. (2018). Estimation of reservoir bio-optical water quality parameters using Smartphone Sensor Apps and Landsat ETM. *Review and Comparative Experimental Results*, Hindawi Journal of Sensors, Article ID 3490757, 32 pages.

Pei, J., Wang, L., Huang, N., Geng, J., Cao, J., & Niu, Z. (2018). Analysis of Landsat-8 OLI Imagery for Estimating Exposed Bedrock Fractions in Typical Karst Regions of Southwest China Using a Karst Bare-Rock Index, *Remote Sens*., 10, 1321; doi:10.3390/rs10091321.

Radaideh, O.M.A., Grasemann, B., Melichar, R., & Mosar, J. (2016). Detection and analysis of morphotectonic features utilizing satellite remote sensing and GIS: An example in SW Jordan, *Geomorphology*, Vol. 275, 58-79.

Rostom, N.G., Shalaby, A.A., Issa, Y.M., & Afifi, A.A. (2017). Evaluation of Mariut Lake water quality using Hyperspectral Remote Sensing and laboratory works, *The Egyptian Journal of Remote Sensing and Space Sciences*, 20, S39–S48.

Ruisi, Z., Min, Z., & Jianping, C. (2011). Study on Geological Structural Interpretation Based on Worldview-2 Remote Sensing Image and Its Implementation, *Procedia Environmental Sciences*, Vol. 10m 653-659.

Saaty, T.L. (1980). The Analytic Hierarchy Process, Mcgraw Hill, Inc. Reprinted By Rws, Publications, Pittsburgh.

Stocklin, J. (1968). Structural history and tectonics of Iran: a review. American Association of Petroleum *Geologists Bulletin*, 52, 1229-1258.

Tripathi, S.C., & India, L. (2014). Remote Sensing Applications in Environmental Research, *Springer International Publishing Switzerland*, 201 P.

Uromeihy, A. (2000). The Lar Dam; an example of infrastructural development in a geologically active karstic region. *Journal of Asian Earth Sciences*, 18: 25-31.

Yu, J., Li, Z., & Yang, L. (2016). Ault system impact on paleokarst distribution in the Ordovician Yingshan Formation in the central Tarim basin, northwest China, *Marine and Petroleum Geology*, Vol. 71, 106-118

Yu, L., Porwal, A., Holden, E.J., & Dentith, M.C. (2012). Towards automatic lithological classification from remote sensing data using support vector machines, *Computers & Geosciences*, Vol. 45, 229-239.